Available online at www.sciencedirect.com
ScienceDirect
Journal of Pharmaceutical and Biomedical Analysis 44 (2007) 477–483
JOURNAL OF PHARMACEUTICAL AND BIOMEDICAL ANALYSIS
www.elsevier.com/locate/jpba

Hyphenated spectroscopy as a polymorph screening tool

Jaakko Aaltonen [a,b,*], Clare J. Strachan [b], Kati Pöllänen [c], Jouko Yliruusi [a], Jukka Rantanen [b,d]

[a] *Division of Pharmaceutical Technology, P.O. Box 56, 00014 University of Helsinki, Finland*
[b] *Drug Discovery and Development Technology Center, P.O. Box 56, 00014 University of Helsinki, Finland*
[c] *Department of Chemical Technology, Lappeenranta University of Technology, P.O. Box 20, 53851 Lappeenranta, Finland*
[d] *Department of Pharmaceutics and Analytical Chemistry, Universitetsparken 2, Faculty of Pharmaceutical Sciences, University of Copenhagen, 2100 Copenhagen, Denmark*

Received 20 November 2006; received in revised form 5 February 2007; accepted 8 February 2007
Available online 13 February 2007

Abstract

Polymorph screening of a model compound (nitrofurantoin) was performed. Nitrofurantoin was crystallized from acetone–water mixtures with varying process parameters. Two anhydrate forms (α and β) and one monohydrate form (II) were crystallized in the polymorph screen. The solid forms were analyzed with three complementary spectroscopic techniques: near-infrared (NIR) spectroscopy, Raman spectroscopy and terahertz pulsed spectroscopy (TPS), and the results of the solid phase analysis were verified with X-ray powder diffraction (XRPD). NIR and Raman spectroscopy were coupled to achieve a rapid and comprehensive method of solid phase analysis. The hyphenated NIR/Raman spectroscopic data were analyzed with a multivariate method, principal component analysis (PCA). The combination was found effective in screening solid forms due to the complementary characteristics of the methods. NIR spectroscopy is powerful in differentiating between anhydrate and hydrate forms and intermolecular features, whereas Raman spectroscopy is sensitive to intramolecular alterations in the molecular backbone.

Keywords: Polymorph screening; Solid phase; Hydrates/solvates; Near-infrared spectroscopy; Raman spectroscopy; Terahertz pulsed spectroscopy; Principal component analysis

1. Introduction

An active pharmaceutical ingredient (API) may exhibit different solid states with no change in molecular structure. This is known as polymorphism, and the different solid states are called polymorphs [1]. Polymorph screening is normally performed during the preformulation stage of drug development. The purpose of the screening is to (a) find the different solid forms the API may exhibit and (b) choose the form most suitable for further development [2]. Even though the screening is called *polymorph* screening, other solid forms (hydrates/solvates and amorphous form) cannot be neglected, since they may possess properties, which make them the best for development. These properties include pharmaceutical and biopharmaceutical properties, such as flowability, compressibility, solubility and bioavailability [3]. Different solid forms of a given API can be patented and therefore be of economic interest, too. On these accounts, comprehensive knowledge of the solid forms of APIs is essential.

Polymorph screening can be approached either experimentally or by computational methods. Even though computational methods have advanced markedly during the last years, experimental work is still needed since the difference in lattice energy between polymorphs can be small making polymorph prediction very challenging [4–5]. Furthermore, crystallization phenomena, especially nucleation, are not yet fully understood [6]. Experimental ways of producing solid forms of APIs include crystallization from a solvent, solvent evaporation, crystallization from the melt and applying mechanical and/or thermal stress. During crystallization from a solvent (the most common way) several issues must be considered. The composition of the solvent, heating/cooling profiles, agitation and seeding are just few of many parameters that can affect the outcome of the crystallization. The scale of the crystallization also plays a

* Corresponding author at: P.O. Box 56 (Viikinkaari 5 E), FI-00014 University of Helsinki, Finland. Tel.: +358 919159159; fax: +358 919159144.
E-mail address: jaakko.aaltonen@helsinki.fi (J. Aaltonen).

0731-7085/$ – see front matter © 2007 Elsevier B.V. All rights reserved.
doi:10.1016/j.jpba.2007.02.009

role and therefore the solid forms successfully generated at very small scale, such as on a chip [7] or self-assembled monolayers (SAMs) [8], cannot always be produced at production scale.

With different crystallization techniques, a large number of samples can easily be produced and analysis during the screening may become a bottleneck. During analysis, the resulting solid forms must first be measured with an established technique and then the data is analyzed. The methods that can be employed are, for example, X-ray powder diffraction (XRPD), optical spectroscopy, solid-state nuclear magnetic resonance spectroscopy (SS-NMR), differential scanning calorimetry (DSC) and thermogravimetry (TG). Optical spectroscopy methods used in solid phase analysis include mid-infrared (IR), near-infrared (NIR), Raman and terahertz pulsed spectroscopy (TPS) [9]. NIR and Raman spectroscopy are reliable and fast methods that require little or no sample preparation and are thus suitable for fast polymorph screening and other process analytical technology (PAT) applications [10–13]. TPS is a new promising technique that has been used for quantitative and qualitative solid phase analysis [14,15]. The solid phase is normally analyzed with more than one of these techniques and the results from different methods are compared. Instead of comparing the results obtained with various techniques, one can benefit from coupling complementary techniques to provide wide-ranging data on the sample in question. These kind of hyphenated methods are widely utilized in chemical analysis [16], but are relatively unusual in physical analysis. The data analysis can be facilitated by multivariate methods. The methods used for pattern recognition include linear approaches (e.g. principal component analysis, PCA) and nonlinear approaches (e.g. artificial neural networks, ANNs) [17].

In this study, experimental polymorph screening was performed on a model compound, nitrofurantoin. NIR and Raman spectroscopy, two complementary spectroscopic methods that have been used individually for polymorph screening [10,12], were used together as a hyphenated technique to obtain fast and extensive solid phase analysis. The spectral data was analyzed using PCA.

2. Experimental

2.1. Crystallization

Raw material, nitrofurantoin ($C_8H_6N_4O_5$, CAS# 67-20-9, anhydrate form β, Sigma–Aldrich Laborchemikalien GmbH, Seelze, Germany) was recrystallized from acetone–water mixtures. Fig. 1 shows the molecular structure of nitrofurantoin. Analytical grade acetone (Sigma–Aldrich Laborchemikalien GmbH Seelze, Germany) and purified water were used. Crystallizations were performed using a 24 well reaction block (H + P Labortechnik GmbH, Oberschleissheim, Germany) and a Huber cc 250 cryostat (Peter Huber Kältemaschinenbau GmbH, Offenburg, Germany). Solutions ($V = 50$ ml) were heated to 55 °C (when all nitrofurantoin had dissolved) and cooled to 10 °C at two different cooling rates (fast rate was 1 °C min^{-1}, slow rate was 0.0375 °C min^{-1}), with and without stirring. In addition to the automated crystallizations, crystallization from pure acetone was also performed as previously reported [18]. The crystals were harvested by vacuum filtration, dried overnight in ambient conditions, and analyzed. Water contents of the acetone–water mixtures and corresponding amounts of nitrofurantoin dissolved are presented in Table 1.

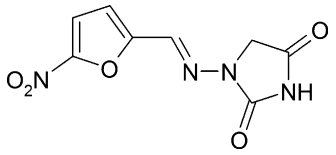

Fig. 1. Molecular structure of nitrofurantoin.

2.2. Methods of analysis

2.2.1. Near-infrared spectroscopy

NIR spectra were measured with a NIR spectrometer (Control Development Inc., South Bend, IN, USA) having a thermoelectrically cooled InGaAs diode array detector, tungsten light source and a fiber optic probe (six illuminating fibers around one collecting fiber). The spectra were collected between 1100 and 2200 nm. Each spectrum was the average of 32 scans.

2.2.2. Raman spectroscopy

Raman spectra were collected using a Raman spectrometer (Control Development Inc., South Bend, IN, USA) equipped with a thermoelectrically cooled CCD detector and a fiber optic probe (RamanProbe RPS785/12-5, InPhotonics, Norwood, MA, USA). A 500 mW laser source emitting 785 nm radiation was used (Starbright 785S, Torsana Laser Technologies, Skodsborg, Denmark). The spectra were recorded between 200 and

Table 1
Water contents of the acetone–water mixtures, corresponding amounts of nitrofurantoin dissolved, and solid forms crystallized in the polymorph screening

Water content of the solvent (v/v)	0%	2%	4%	10%	17%	20%	25%	33%	50%	67%	75%
Amount of nitrofurantoin (mg/ml)		9	12	12	12	11	11	8	4	1.5	1
Resulting solid forms	β[a]	α/β[b], II[c]	II[c,d], α[e]				II				

[a] Method described by Pienaar et al. [18].
[b] With stirring.
[c] Without stirring.
[d] Fast cooling with stirring.
[e] Slow cooling with stirring.

2200 cm^{-1}, and were the average of five scans with an integration time of 3 s. Both NIR and Raman spectra were collected using a rotating sample holder to avoid sub-sampling.

To aid interpretation of the Raman spectra, quantum chemical modeling was performed on the nitrofurantoin single molecule. The conformation of the molecule was optimized and then the Raman frequencies and activities calculated using density functional theory calculations (B3LYP functional, 6-31G(d) basis set). Calculations were performed using the Gaussian 03 software [19]. Modes were visualised using the GaussView package that accompanies Gaussian 03.

2.2.3. Terahertz pulsed spectroscopy

Terahertz pulsed spectra were recorded using a TPSspectra1000 V spectrometer (TeraView, Cambridge, UK). Samples were mixed with polyethylene (Induchem, Volketwil, Switzerland, particle size <10 μm) and pressed into a disc. Spectra were recorded at room temperature while the sample chamber was purged with dry nitrogen. Each spectrum was the average of 1800 scans (1 min measuring time) and recorded from 2 to 130 cm^{-1} with a spectral resolution of 1 cm^{-1}. Blackman–Harris 3-term apodization was used for the Fourier transformation and absorbance spectra were calculated using a polyethylene disc as a reference.

2.2.4. Crystal structure verification

The XRPD patterns of the crystals were measured with a theta–theta X-ray powder diffractometer (D8 Advance, Bruker AXS GmbH, Karlsruhe, Germany). Measurements were performed in symmetrical reflection mode with Cu Kα radiation (λ = 1.54 Å) using Göbel mirror. The range measured was 5–40° (2θ), with steps of 0.05° (time per step was 1 s). Crystal structures were verified by comparing the experimental XRPD patterns to the structures of nitrofurantoin [18,20] reported in the Cambridge Structural Database (CSD) [21].

2.2.5. Processing and multivariate analysis of NIR/Raman hyphenated spectra

NIR and Raman spectroscopy were used together as a hyphenated technique for polymorph screening. TPS was not used in tandem with NIR and Raman spectroscopy since currently, the technique cannot be considered a high-throughput polymorph screening method.

The NIR spectral region of 1300–2050 nm and the Raman spectral region of 645–1745 cm^{-1} were used for multivariate data analysis. Other parts of the spectra were discarded since they contained mainly noise. The selected regions of the NIR and Raman spectra were treated with standard normal variate (SNV) transformation to remove baseline and intensity differences due to size, habit and optical properties of the crystals. In SNV transformation, each spectrum is normalized by the standard deviation of the responses within the whole spectral range [22]. The SNV transformed NIR and Raman spectra of each sample were merged into one array, and thereafter the merged spectra were centered and analyzed with PCA using Simca-P 10.5 software (Umetrics AB, Umeå, Sweden).

In PCA, the data matrix **X** is decomposed to:

$$\mathbf{X} = \mathbf{TP}' + \mathbf{E}$$

where **T** is the score matrix describing the samples, **P** is the loading matrix describing the variables and **E** is the residual matrix. Each combination of score and loading vectors included in the **TP′** matrix constitute a principal component (PC), with the first PC describing the largest amount of variation in the data set. To visualize spectral differences, the scores of different PCs can be plotted against one another in a scatter plot. The samples that are similar and hence have closely matching spectra will be located in one cluster while samples that contain differences form separate clusters. The loadings of a certain component define the importance of each variable in the formation of that component. The first two or three principal components extracted from the data can often be used to interpret the main phenomena in the data since these components usually contain most of the systematic variation present in the data.

3. Results And discussion

3.1. Crystal structure verification with XRPD

Two anhydrate forms (α and β; CSD refcodes LABJON01 and LABJON02, respectively) [18] and one monohydrate form (II; CSD refcode HAXBUD) [20] of nitrofurantoin were crystallized in the polymorph screen. XRPD patterns of the three forms are presented in Fig. 2. The XRPD verified crystal forms of the samples and corresponding crystallization conditions are presented in Table 1. As expected, the water content of the solvent most affected the outcome of the crystallization. With water contents above 4%, the resulting crystal form was always form II, regardless of cooling rate or stirring. Interestingly, at low water contents (2% and 4%) hydrate formation could be controlled by the stirring and cooling rate. At a water content of 2%, the unstirred crystallizations yielded crystals of form II, but stirring induced formation of form α or β. With a water content of 4%, a combination of slow cooling and stirring produced crystals of form α, whereas crystallizations with fast cooling and stirring resulted in form II. These results underline the need to also examine the effects of various processing parameters during polymorph screening. However, investigation of the complex overlapping phenomena determining the final solid form was beyond the scope of this article.

3.2. Spectroscopic characterization of solid forms

The solid forms created in the screening crystallizations were investigated with three complementary spectroscopic techniques, near-infrared, Raman and terahertz pulsed spectroscopy. The different characteristics of these methods enable thorough solid phase examination.

3.2.1. Near-infrared spectroscopy

Fig. 3a shows NIR spectra of the three crystallized forms. The NIR spectrum of form II contains dominant features related

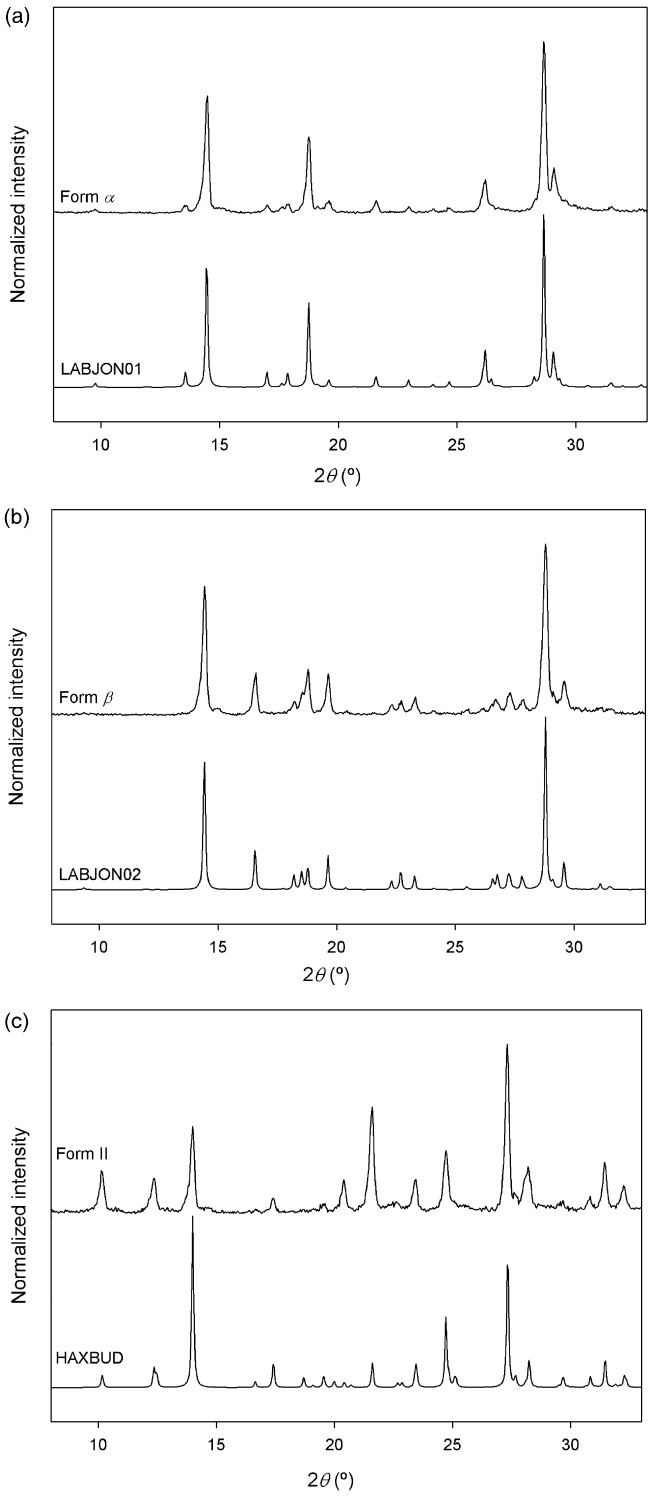

Fig. 2. XRPD patterns of the solid forms crystallized in the polymorph screening (above) and corresponding theoretical patterns calculated from the single-crystal structures (below). (a) Form α; (b) form β; and (c) form II.

to O–H bonding at 1416 nm in the first overtone region, and 1920 nm and 1974 nm in the combination band region. These features are mostly due to the presence of water molecules in the crystal lattice. The NIR spectra of all three forms contain bands in the region 1600–1750 nm (C–H vibrations in the first overtone region) characteristic of the molecular structure. Regardless of the common bands mentioned, the anhydrate forms α and β have differences in the intermolecular bonding. In the crystal structure of form α, nitrofurantoin molecules associate in a "head-to-head" arrangement forming centrosymmetric "dimers" through two identical intermolecular hydrogen bonds, whereas in form β every molecule is connected to two other molecules instead of one [18]. The differences between the two forms are indicated by the bands at 1551 nm and 1987 nm, representing vibrations in the 1st overtone and combination band region in the NIR spectrum of form β, respectively.

3.2.2. Raman spectroscopy

The Raman spectra mainly represent intramolecular vibrations of the drug molecule. These vibrations can be affected by changes in molecular conformation and molecular bonding. The Raman spectra are distinct for each of three crystallized forms of nitrofurantoin (Fig. 3b). The quantum chemical calculations revealed that one of the strongest modes mainly represents an in-phase NO_2 stretch, and this occurs at 1343 cm^{-1} for form α, 1349 cm^{-1} for form β and 1345 cm^{-1} for form II. This mode is affected by different intermolecular distances between the O atoms in the NO_2 group and H atoms in the furan and hydantoin moieties of neighboring molecules. In form II a short contact between the O atom of the NO_2 group and the H atom in the water molecule is observed. Bands associated with furan ring vibrations were also different for the three forms. One such band occurred at 1016 cm^{-1} for form α and 1018 cm^{-1} for form β but was blue-shifted to 1025 cm^{-1} for form II. An intense band appeared at 1611 cm^{-1} and 1609 cm^{-1} for forms α and β, respectively, and was shifted to 1615 cm^{-1} for form II. This is predominantly associated with stretching of the C=N linkage between the nitrofuran and hydantoin moieties.

3.2.3. Terahertz pulsed spectroscopy

The three forms of nitrofurantoin show distinct terahertz pulsed spectra, and the peaks observed can be attributed to crystalline phonon modes (Fig. 3c). In the form II spectrum, the most prominent features peak at 102 cm^{-1} and 111 cm^{-1}. These are probably two separate modes, however, this is not certain since the signal-to-noise ratio of the spectra is significantly decreased above 100 cm^{-1}. Much weaker features include distinct peaks at 21 cm^{-1} and 34 cm^{-1}, and shoulders at 48 cm^{-1}, 55 cm^{-1} and 76 cm^{-1} and 87 cm^{-1}. Form α exhibits relatively few modes; the largest mode occurs at 99 cm^{-1}, with other modes present at 40 cm^{-1} and 81 cm^{-1}. In the form β spectrum a single peak occurs at 65 cm^{-1}, and a large feature peaks at 88 cm^{-1} which may also consist of additional overlapping modes at slightly higher wavenumbers.

At present these modes cannot be assigned to specific phonon vibrations. Work to improve interpretation of these modes using computational chemistry is in its infancy, but it is likely that in future specific phonon vibrations can be assigned to these peaks [23]. Despite the present difficulties in interpreting terahertz spectra, the differences between the spectra of the three nitrofurantoin forms show that TPS is another potential spec-

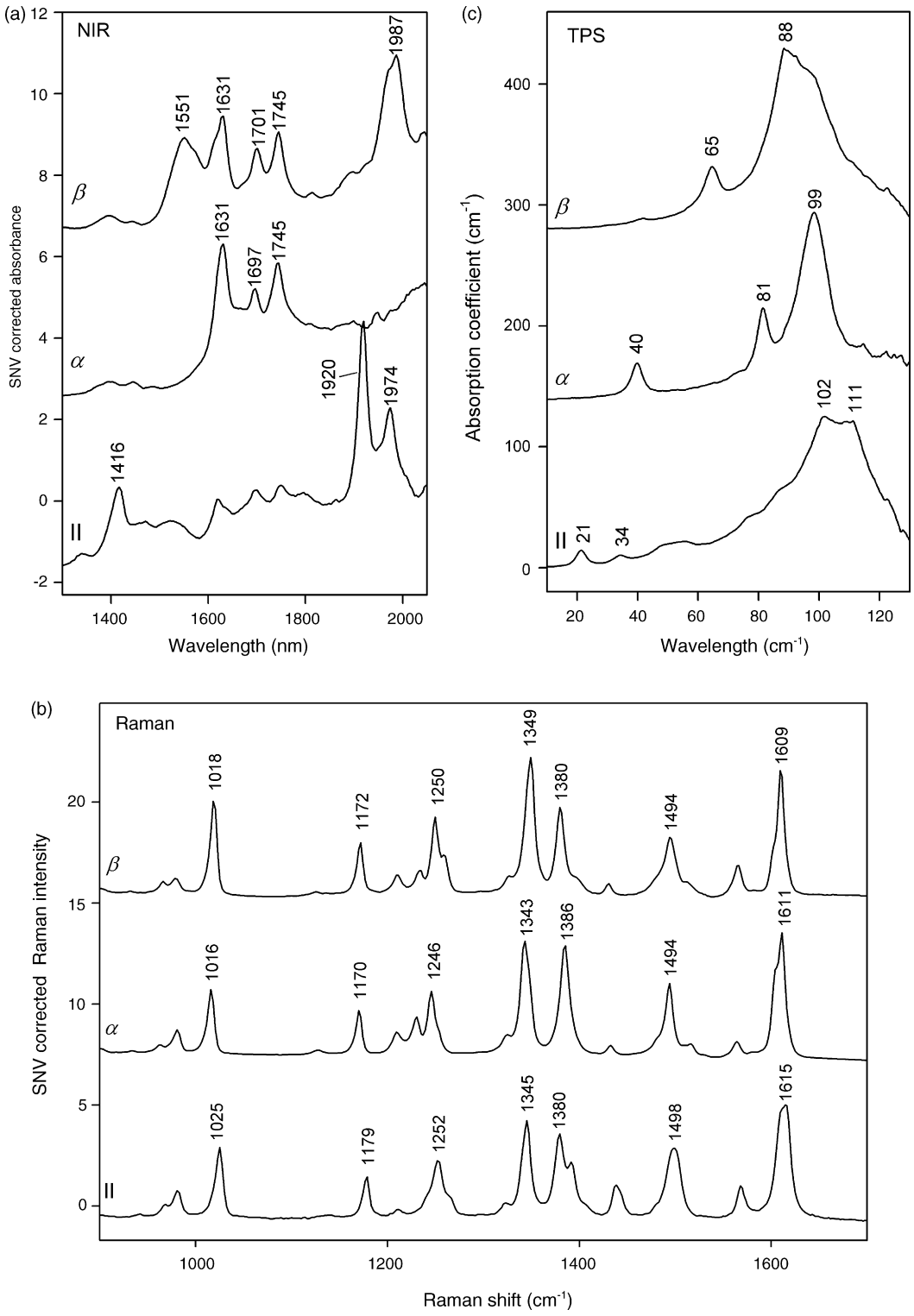

Fig. 3. Spectroscopic characterization of solid forms II, α and β of nitrofurantoin. (a) NIR spectra; (b) Raman spectra; (c) TPS spectra. The spectra are offset for clarity.

troscopic tool that may be used for polymorph screening. Furthermore, TPS has been able to differentiate structurally similar polymorphs, which could not be differentiated using other spectroscopic methods [24]. However, with current set-ups TPS cannot be considered as a high throughput method.

3.3. Polymorph screening with hyphenated spectroscopy

Three clusters were clearly separated in the score plot of the PCA (Fig. 4). The clusters represent the different solid forms verified by XRPD. The first principal component (PC1) explained

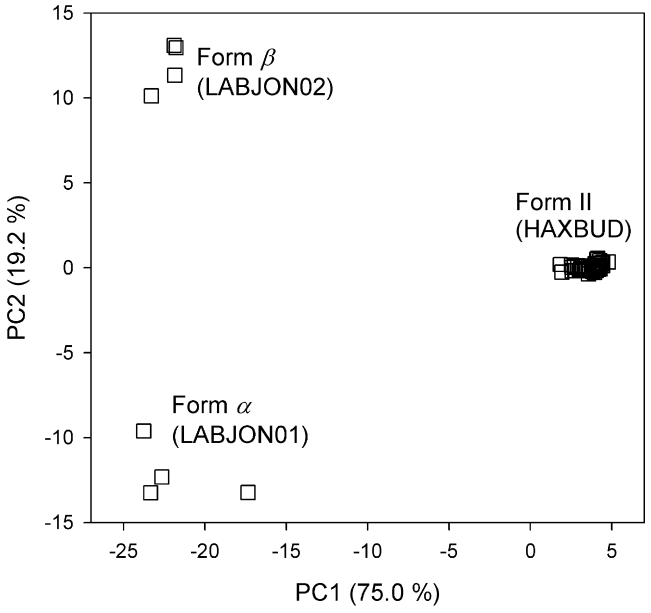

Fig. 4. The score plot of the PCA of the SNV corrected, merged and centered NIR/Raman spectra. The three clusters represent crystal forms II (CSD refcode HAXBUD), α (LABJON01) and β (LABJON02) of nitrofurantoin. PC1 and PC2 together explained 94% of the NIR/Raman spectral variation.

75% of the spectral variation and separated the monohydrate from the anhydrate forms. The second principal component (PC2) explained 19% of the spectral variation and separated the two anhydrate forms from each other.

The loadings represent the intrinsic nature of NIR and Raman spectra. NIR spectral loading plots have broad peaks whereas those of Raman spectra are narrow and sharp. The features that separate form II from α and β are clearly visible in the NIR spectral loadings of PC1 (Fig. 5). PC1 has the most important loading values in the NIR region at 1416 and 1920 nm, which correspond to the presence of water molecules in form II. The main negative loading at 1631 nm corresponds to the band characteristic of forms α and β but not of form II, further separating the anhydrate forms from the monohydrate. In the Raman loadings of PC1, bands at 1016–1025 cm^{-1} and 1609–1615 cm^{-1} had high values separating form II from α and β. The highest PC2 loadings in the NIR spectral range were observed between 1500 and 1600 nm, and between 1940 and 2020 nm. The most important loadings of PC2 were observed in the Raman spectral region between 1343 and 1349 cm^{-1}. The areas highlighted by the PC2 loadings are those with the largest differences between the NIR and Raman spectra of forms α and β.

The number of principal components used for clustering was determined on the basis of what was seen in the loadings and the R^2 and Q^2 values of the PCA. The addition of a third principal component (PC3) did not bring in any meaningful information according to the loadings of PC3 (not shown). This, combined with the investigation of the contribution of PC3 to the R^2 and Q^2 values of the PCA (2.4% and 0.6%, respectively), showed that using more than two PCs was not reasonable and might cause overfitting of the data.

The rationale behind the combination of NIR and Raman spectroscopy is that they are fast methods that require no or very little sample preparation and are suitable for high throughput polymorph screening. Furthermore, they are complementary. Raman spectroscopy detects symmetric vibrations of nonpolar groups (mainly C–C), while NIR spectroscopy detects antisymmetric vibrations of polar groups (mainly O–H, C–H and N–H). Thus, Raman spectroscopy is more sensitive to alterations in the molecular backbone whereas NIR spectroscopy can detect differences in the hydrogen bonding networks between the drug molecules and possible adducts (such as solvent molecules) in the crystal lattice. The presence of water molecules is easily detected with NIR spectroscopy, whereas water is a very weak Raman scatterer. When combined, these complementary methods provide a more comprehensive method for solid phase analysis. The current state of the art is to use non-invasive spectroscopic methods in high throughput polymorph screening. Both NIR and Raman spectroscopic measurements can be performed from small amount of material, even from a few crystals on a well plate. Combining the information from both these methods increases the likelihood of identification of all new solid forms of an API.

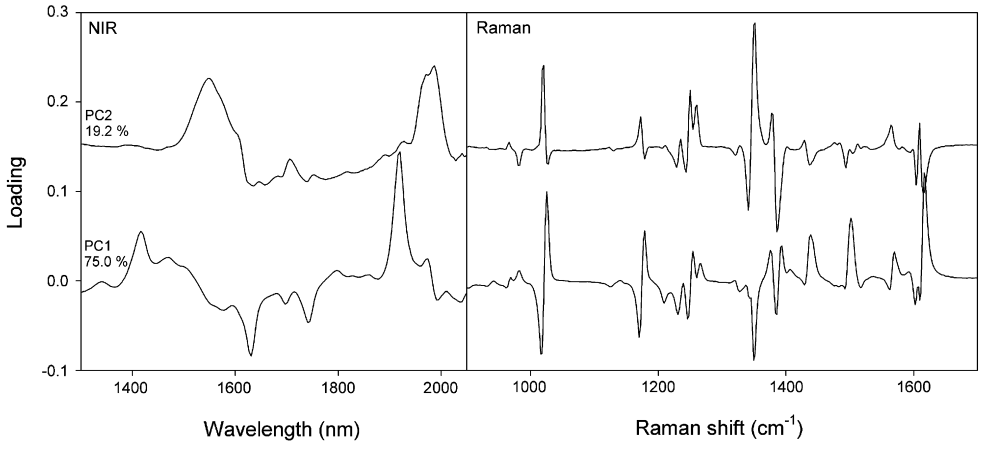

Fig. 5. The loadings of PC1 and PC2.

4. Conclusions

A polymorph screening study with a model compound, nitrofurantoin, was performed. In the screening, three solid forms (monohydrate form II, and anhydrates α and β) were found and verified with X-ray powder diffraction. Critical process parameters affecting the polymorphic outcome were also found. The three solid forms were characterized and differentiated with near-infrared, Raman and terahertz pulsed spectroscopy. Hyphenated NIR/Raman spectroscopy combined with principal component analysis was utilized as a fast and comprehensive method of solid phase analysis. The hyphenated method was found powerful in differentiating between the solid forms. Near-infrared spectroscopy was effective in separating the hydrate form (II) from the anhydrates (α and β), while Raman spectroscopy provided accurate information from the differences between the anhydrates.

Acknowledgements

The authors would like to thank Axel Zeitler and TeraView Ltd. for use of the TPSspectra1000 V spectrometer and assistance with measurements. Sarah Howell is thanked for help with quantum chemical calculations. Thanks to Morten Allesø for very fruitful discussions throughout the course of this work. The Academy of Finland (decision 107343), Finnish Cultural Foundation (Elli Turunen fund), Graduate School in Pharmaceutical Sciences (Finland) and Drug Research Academy (Faculty of Pharmaceutical Sciences, University of Copenhagen) are acknowledged for financial support.

References

[1] J. Bernstein, Polymorphism in Molecular Crystals, Oxford University Press, Oxford, UK, 2002.
[2] R. Hilfiker, S.M. De Paul, M. Szelagiewcz, in: R. Hilfiker (Ed.), Polymorphism in the Pharmaceutical Industry, WILEY-VCH Verlag GmbH & Co., Weinheim, Germany, 2006, pp. 287–308.
[3] J. Haleblian, W. McCrone, J. Pharm. Sci. 58 (1969) 911–929.
[4] W.I. Cross, N. Blagden, R.J. Davey, R.G. Pritchard, M.A. Neumann, R.J. Roberts, R.C. Rowe, Cryst. Growth. Des. 3 (2003) 151–158.
[5] S.L. Price, Adv. Drug. Del. Rev. 56 (2004) 301–319.
[6] R.J. Davey, Nature 428 (2004) 374–375.
[7] T. Lee, T. Hung, C.S. Kuo, Pharm. Res. 23 (2006) 2542–2555.
[8] A.Y. Lee, I.S. Lee, S.S. Dette, J. Boerner, A.S. Myerson, J. Am. Chem. Soc. 127 (2005) 14982–14983.
[9] R. Hilfiker (Ed.), Polymorphism in the Pharmaceutical Industry, WILEY-VCH Verlag GmbH & Co., Weinheim, Germany, 2006.
[10] M.L. Peterson, S.L. Morissette, C. McNulty, A. Goldsweig, P. Shaw, M. LeQuesne, J. Monagle, N. Encina, J. Marchionna, A. Johnson, J. Gonzalez-Zugasti, A.V. Lemmo, S.J. Ellis, M.J. Cima, Ö. Almarsson, J. Am. Chem. Soc. 124 (2002) 10958–10959.
[11] R. Hilfiker, J. Berghausen, F. Blatter, A. Burkhard, S.M. De Paul, B. Freiermuth, A. Geoffroy, U. Hofmeier, C. Marcolli, B. Siebenhaar, M. Szelagiewicz, A. Vit, M. von Raumer, J. Therm. Anal. Calorim. 73 (2003) 429–440.
[12] J. Aaltonen, J. Rantanen, S. Siiriä, M. Karjalainen, A. Jørgensen, N. Laitinen, M. Savolainen, P. Seitavuopio, M. Louhi-Kultanen, J. Yliruusi, Anal. Chem. 75 (2003) 5267–5273.
[13] PAT—A Framework for Innovative Pharmaceutical Development, Manufacturing, and Quality Assurance, U.S. Food and Drug Administration, Rockville, MD. 2004.
[14] P.F. Taday, I.V. Bradley, D.D. Arnone, M. Pepper, J. Pharm. Sci. 92 (2003) 831–838.
[15] C.J. Strachan, P.F. Taday, D.A. Newham, K.C. Gordon, J.A. Zeitler, M. Pepper, T. Rades, J. Pharm. Sci. 94 (2005) 837–846.
[16] C. Pan, F. Liu, Q. Ji, W. Wang, D. Drinkwater, R. Vivilecchia, J. Pharm. Biomed. Anal. 40 (2006) 581–590.
[17] M. Daszykowski, B. Walczak, D.L. Massart, Chemom. Intell. Lab. Syst. 65 (2003) 97–112.
[18] E.W. Pienaar, M.R. Caira, A.P. Lötter, J. Crystallogr. Spectrom. Res. 24 (1993) 785–790.
[19] M.J. Frisch, G.W. Trucks, H.B. Schlegel, G.E. Scuseria, M.A.C. Robb, J.R.J. Montgomery, J.A.T. Vreven, K.N. Kudin, J.C. Burant, J.M. Millam, S.S. Iyengar, J. Tomasi, V. Barone, B. Mennucci, M. Cossi, G. Scalmani, N. Rega, G.A. Petersson, H. Nakatsuji, M. Hada, M. Ehara, K. Toyota, R. Fukuda, J. Hasegawa, M. Ishida, T. Nakajima, Y. Honda, O. Kitao, H. Nakai, M. Klene, X.Li, J.E. Knox, H.P. Hratchian, J.B. Cross, V. Bakken, C. Adamo, J. Jaramillo, R. Gomperts, R.E. Stratmann, O. Yazyev, A.J. Austin, R. Cammi, C. Pomelli, J.W. Ochterski, P.Y. Ayala, K. Morokuma, G.A. Voth, P. Salvador, J.J. Dannenberg, V.G. Zakrzewski, S. Dapprich, A.D. Daniels, M.C. Strain, O. Farkas, D.K. Malick, A.D. Rabuck, K. Raghavachari, J.B. Foresman, J.V. Ortiz, Q. Cui, A.G. Baboul, S. Clifford, J. Cioslowski, B.B. Stefanov, G. Liu, A. Liashenko, P. Piskorz, I. Komaromi, R.L. Martin, D.J. Fox, T. Keith, M.A. Al-Laham, C.Y. Peng, A. Nanayakkara, M. Challacombe, P.M.W. Gill, B. Johnson, W. Chen, M.W. Wong, C. Gonzalez, J.A. Pople. Gaussian 03, Revision C.02. Gaussian Inc., Wallingford CT, 2004.
[20] E.W. Pienaar, M.R. Caira, A.P. Lötter, J. Crystallogr. Spectrom. Res. 23 (1993) 739–744.
[21] F.H. Allen, Acta. Cryst. B58 (2002) 380–388.
[22] R.J. Barnes, M.S. Dhanoa, S.J. Lister, Appl. Spectrosc. 43 (1989) 772–777.
[23] G.M. Day, J.A. Zeitler, W. Jones, T. Rades, P.F. Taday, J. Phys. Chem. B 110 (2006) 447–456.
[24] J.A. Zeitler, D.A. Newnham, P.F. Taday, T. Threlfall, R.W. Lancaster, R.W. Berg, C.J. Strachan, M. Pepper, K.C. Gordon, T. Rades, J. Pharm. Sci. 95 (2006) 2486–2498.